ACS SyntheticBiology

Research Article

pubs.acs.org/synthbio

A Set of Versatile Brick Vectors and Promoters for the Assembly, Expression, and Integration of Synthetic Operons in *Methylobacterium extorquens* AM1 and Other Alphaproteobacteria

Lennart Schada von Borzyskowski,[†] Mitja Remus-Emsermann,[†] Ramon Weishaupt,[‡] Julia A. Vorholt, and Tobias J. Erb*

Institute of Microbiology, Eidgenössische Technische Hochschule (ETH) Zurich, Vladimir-Prelog-Weg 4, 8093 Zurich, Switzerland

Supporting Information

ABSTRACT: The discipline of synthetic biology requires standardized tools and genetic elements to construct novel functionalities in microorganisms; yet, many model systems still lack such tools. Here, we describe a novel set of vectors that allows the convenient construction of synthetic operons in *Methylobacterium extorquens* AM1, an important alphaproteobacterial model organism for methylotrophy and a promising platform organism for methanol-based biotechnology. In addition, we provide a set of constitutive alphaproteobacterial promoters of different strengths that were characterized in detail by two approaches: on the single-cell scale and on the cell population level. Finally, we describe a straightforward strategy to deliver synthetic constructs to the genome of *M. extorquens* AM1 and other Alphaproteobacteria. This study defines a new standard to systematically characterize genetic parts for their use in *M. extorquens* AM1 by using single-cell fluorescence microscopy and opens the toolbox for synthetic biological applications in *M. extorquens* AM1 and other alphaproteobacterial model systems.

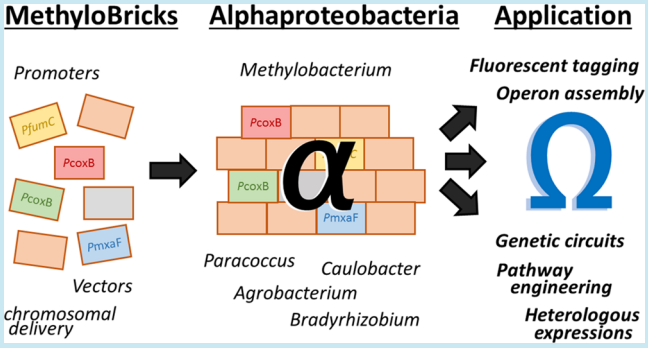

KEYWORDS: *Alphaproteobacteria, biobricks, vector system, operon assembly, promoter library, Caulobacter, Agrobacterium, Paracoccus*

The discipline of synthetic biology integrates concepts of engineering, such as abstraction, standardization, and modularity, into classical biology[1] and is aimed at modulating[2] or even creating *de novo* biological functionalities in living systems.[3] These tasks require a toolset of well-characterized, standardized, and reusable genetic elements that are optimized for the host organism of choice. Such building blocks include plasmid backbones, selection markers, promoters, terminators, ribosome binding sites (RBS), and open reading frames (ORFs). Genetic elements must comply with certain standards to meet the aforementioned requirements, such as the BioBrick standard.[4] To date, almost 10 000 genetic elements complying with this standard are cataloged in the Registry of Standard Biological Parts (partsregistry.org) and have been employed in numerous successful projects mainly in *Escherichia coli*, e.g. for, such as the construction of pollutant-detecting bacterial cells,[5] the bacterial production of even-chain alkanes,[6] and the development of RBS-linked toggle switches.[7] Tools compatible with the BioBrick standard have been recently developed for other organisms, such as *Corynebacterium glutamicum*,[8] *Bacillus subtilis*[9] or the plant model organism *Arabidopsis thaliana*.[10] However, similar standardized BioBrick toolsets are still lacking for many other bacterial model systems, especially those of biotechnological relevance.

In recent years, the concept of a methanol-based biotechnology has garnered considerable interest. This concept makes use of methanol as the carbon source for methanol-utilizing microorganisms, so-called methylotrophs. Methanol can be synthesized from natural gas, which makes it an interesting raw material for biotechnological processes because chemically synthesized methanol does not directly compete with food crops. Thus, it provides an alternative supply to the classical ethanol- and sugar-based biotechnology.[11] Methanol has already been successfully applied for the industrial-scale production of single-cell protein in the 1970s;[12] however, current efforts have shifted to the production of fine chemicals from methanol in microbial cell factories,, the most prominent example of which being the European research initiative PROMYSE (seventh FWP, KBBE.2011.3.6-04). The key model organism for methylotrophy and methanol-based biotechnology is the Alphaproteobacterium *Methylobacterium extorquens* AM1.[13,14] Besides using methanol as its carbon source, the organism can also grow on several C2, C3, and C4 compounds as its sole source of carbon and energy. The genomes of *M. extorquens* AM1 and six related strains have

Received: March 22, 2014
Published: July 23, 2014

   dx.doi.org/10.1021/sb500221v | *ACS Synth. Biol.* 2015, 4, 430−443

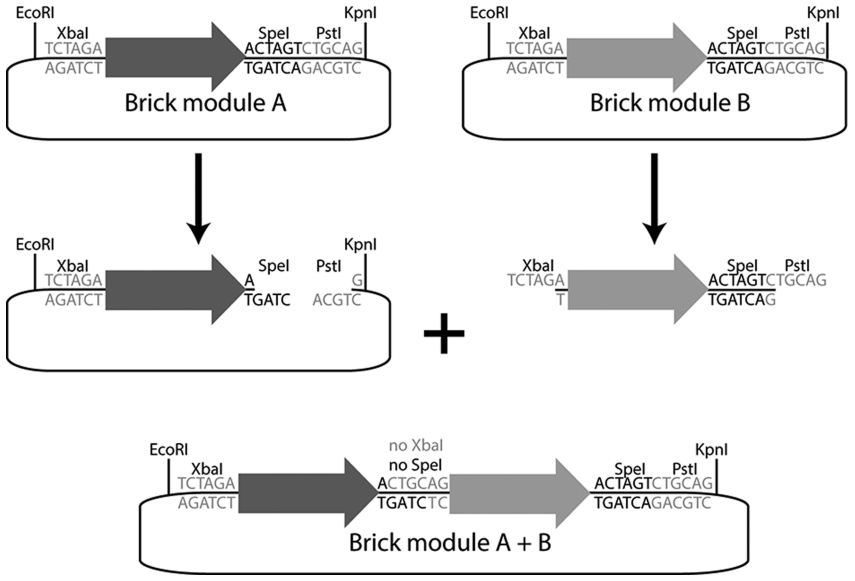

Figure 1. Methylobrick cloning scheme. Methylobrick module A carrying a promoter sequence (dark gray) and Methylobrick module B carrying a gene (light gray) to be expressed in *M. extorquens* AM1. Methylobrick module B is combined with Methylobrick module A using isocaudomeric restriction, by digesting module A with SpeI and PstI and module B with XbaI and PstI. The overhangs of XbaI and SpeI are ligated by deleting both restriction sites and creating a "scar". The SpeI/PstI site downstream of the combined modules allows the addition of further modules and the generation of polycistronic operons.

been fully sequenced, and many more genomes are waiting to be closed.[15−17] A genome-scale metabolic network was reconstructed that allows the systems analysis of *M. extorquens* AM1 metabolism and provides the basis for its rational remodeling and the design of new synthetic pathways.[18]

For basic applications in *M. extorquens* AM1, a genetic toolkit and specialized vectors have been developed[19,20] that were successfully used for homo- and heterologous gene expression in this organism.[14,21−24] However, many well-characterized promoters commonly used in *Escherichia coli* are either not functional in *M. extorquens* AM1 (e.g., *λ*PL and *P*R) or promote only low-level protein expression (e.g., *P*lac). Therefore, gene expression in *M. extorquens* AM1 has almost exclusively been driven by the strong promoter region of the *mxaF* gene (*P*mxaF) that encodes the large subunit of methanol dehydrogenase, which represents up to 9% of the total soluble protein in *M. extorquens* AM1 under methylotrophic growth conditions.[25] Only very recently has the similarly strong promoter *P*R from the rhizobial phage 16−3 (*P*R,16−3) been introduced for gene expression in *M. extorquens* AM1.[26] Inducibility of gene expression was achieved by combining these promoters with regulatory elements, such as the CymR or TetR repressor.[26,27]

All of these genetic tools for *M. extorquens* AM1 have proven to be valuable, but they represent adaptions to specific needs or stand-alone solutions. The construction of synthetic pathways in *M. extorquens* AM1, however, requires a more systematic set of tools and standardized parts. Here, we introduce a vector system that allows for the easy assembly of multiple genes and other genetic elements for their use in *M. extorquens* AM1. These Methylobrick vectors are restriction site compatible with well-established vector expression systems (such as the pET series from Novagen) as well as with the BioBrick system. Moreover, we provide a novel set of constitutive promoters of different strengths for the stable expression of genes in *M. extorquens* AM1 and other alphaproteobacterial species. To evaluate the strength and variability of these promoters, we established a simple readout based on fluorescence that allows promoter characterization on the single-cell level and that we propose as a standard procedure for future characterizations of novel promoter and regulatory elements in *M. extorquens* AM1. Finally, we provide a second vector system that enables the stable integration of synthetic operons into the genome of *M. extorquens* AM1 (and other Alphaproteobacteria) through Tn5 delivery. In summary, this toolbox of vectors and genetic elements provides the basis for the future implementation of artificial, fine-tuned metabolic pathways in *M. extorquens* AM1 (and other Alphaproteobacteria), which is indispensable for the realization of the biotechnological potential of these organisms.

RESULTS AND DISCUSSION

Construction of Methylobrick Vectors for the Convenient Assembly of Genetic Parts. To allow for the standardized cloning and assembly of genetic parts and synthetic operons for expression in *M. extorquens* AM1, we designed a multiple cloning site (MCS) based on the following criteria: (1) the use of the best combinations of isocaudomeric restriction sites flanking the MCS that enable the sequential assembly of genetic elements by isocaudomeric cloning and that are compatible with the BioBrick system, (2) a RBS optimized for expression in Alphaproteobacteria upstream of the MCS, (3) a maximum number of restriction sites within the MCS that are compatible with established vector systems (notably, the pET and pSEVA[28] vector series), and (4) an optimized sequence downstream of the MCS that contains stop codons in three reading frames. The MCS was introduced into the previously described vectors pCM80[20] and pLM01[29] to create the two basic promoterless brick vectors, pTE100 and pTE101, that confer resistance to tetracycline and kanamycin, respectively. Once introduced into the MCS, two genetic elements can be readily combined by isocaudomeric cloning either by using the isocaudomers XbaI and SpeI (forward assembly) or the isocaudomers BsrGI and Acc65I (reverse assembly). For standard brick cloning in the forward direction,

dx.doi.org/10.1021/sb500221v | *ACS Synth. Biol.* 2015, 4, 430−443

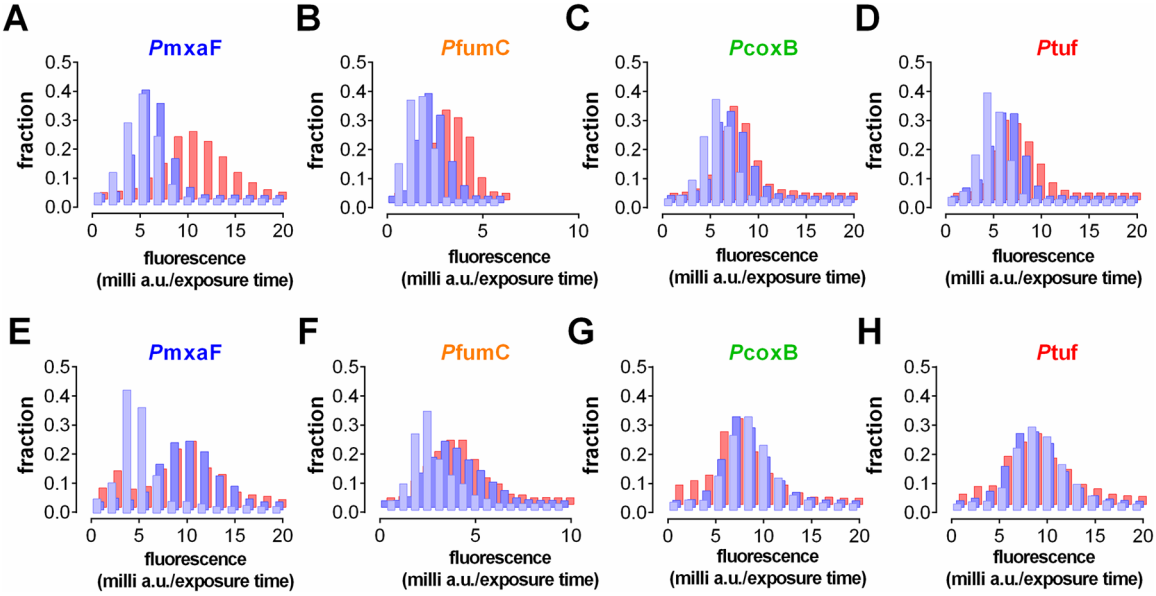

Figure 2. Single-cell fluorescence of promoters *P*mxaF, *P*fumC, *P*coxB, and *P*tuf with the GFPmut3 reporter during different growth phases of *M. extorquens* AM1 in two different media. The GFP fluorescence of a minimum of 400 individual cells of *M. extorquens* AM1 carrying pTE102-GFPmut3 (A, E), pTE103-GFPmut3 (B, F), pTE104-GFPmut3 (C, G), or pTE105-GFPmut3 (D, H) was assessed during different growth stages in minimal medium (early exponential phase, light blue bars; mid-exponential phase, dark blue bars; stationary phase, red bars) that contained either methanol (A–D) or succinate (E–H) as the sole carbon source. The fraction of the total cell population is given with respect to the fluorescence in milli absorption units (a.u.) per exposure time.

the host vector carrying the future upstream genetic element is opened by digesting 5′ with SpeI and 3′ with either PstI, KpnI, or SbfI before being combined with a downstream fragment that was excised from the donor vector using 5′ XbaI and 3′ the same restriction enzyme that was used to open the host vector (PstI, KpnI, or SbfI). This scars the former restriction sites for XbaI and SpeI after ligation, which enables the further addition of novel elements downstream, as depicted in Figure 1.

Identification and Molecular Characterization of a Basic Methylobrick Promoter Set. Many well-characterized promoters of *E. coli* are not functional in *M. extorquens* AM1. Thus, we selected four different promoters from the genome of *M. extorquens* AM1 to drive constitutive expression from Methylobrick vectors. Besides the previously characterized promoter region *P*mxaF, the putative promoter regions of three genes, *fumC* coding for a fumarase (MexAM1_METAp2857), *coxB* coding for the cytochrome *c* oxidase subunit II (MexAM1_META1p3474), and EF-Tu coding for the translation elongation factor thermo-unstable (MexAM1_METAp4832), further referred to as *P*fumC, *P*coxB, and *P*tuf, respectively, were chosen for further characterization. All three putative promoters were expected to be constitutively expressed, as deduced from transcriptomics studies of *M. extorquens* AM1 with microarrays[30] and RNA-Seq (unpublished data, Francez-Charlot and Vorholt).

The four different promoter regions were inserted into the basic brick vectors to allow expression of genes and operons introduced downstream by isocaudomeric cloning. This procedure created pTE102, pTE103, pTE104, and pTE105 containing *P*mxaF, *P*fumC, *P*coxB, and *P*tuf, respectively (Table 3). In order to verify that the core regions of the three novel promoters were present in plasmids pTE103–105 and to enable the application of these promoters as genetic elements in constructs including a minimal promoter region, we determined the start of the 5′-untranslated regions (5′-UTR) of the three mRNA transcripts from RNA-Seq data as well as through transcription start site mapping by 5′-RACE (rapid amplification of cDNA ends).[31] Both approaches yielded consistent results for the 5′-UTRs of all three genes (*fumC*, *coxB*, and *tuf*). These results were also generally in line with *in silico* analyses of the core promoter regions by the BPROM software[32] (www.softberry.com), according to which the −35/−10 boxes were predicted at an approximate distance upstream of the experimentally determined transcriptional start sites (see Supporting Information Figure S1).

Quantification of Methylobrick Promoter Activities and Intrapopulation Variability in Different Growth Phases on the Single-Cell Level. To quantify the promoter activities of *P*mxaF, *P*coxB, *P*fumC, and *P*tuf in the Methylobrick vectors, the expression level of fluorescent proteins was chosen as a readout.[33,34] To account for intrapopulation variability or potential heterogeneity of gene expression, we decided to analyze all promoter activities on the single-cell level.[35] To that end, the fluorescent proteins GFPmut3,[36] eYFP,[37] and mCherry[38] were cloned into pTE100 to create pTE100-GFP, pTE100-eYFP, and pTE100-mChe, respectively (Table 3). pTE100-GFPmut3 and pTE100-mCherry were subsequently used as donors, i.e., reporter modules, for integration into promoter modules pTE102, pTE103, pTE104, and pTE105 (Figure 1). The resulting reporter constructs, containing both a promoter and a fluorescent reporter, were then transformed into *M. extorquens* AM1.

First, we tested the growth phase-dependent behavior of promoter activities with the GFP-reporter constructs on two standard minimal media that are typically used for cultivation of *M. extorquens* AM1 and that are either based on methanol or succinate as the sole carbon source. For that, the single-cell fluorescence of *M. extorquens* AM1 strains each containing one of the GFP-based reporter plasmids was analyzed during

dx.doi.org/10.1021/sb500221v | *ACS Synth. Biol.* 2015, 4, 430–443

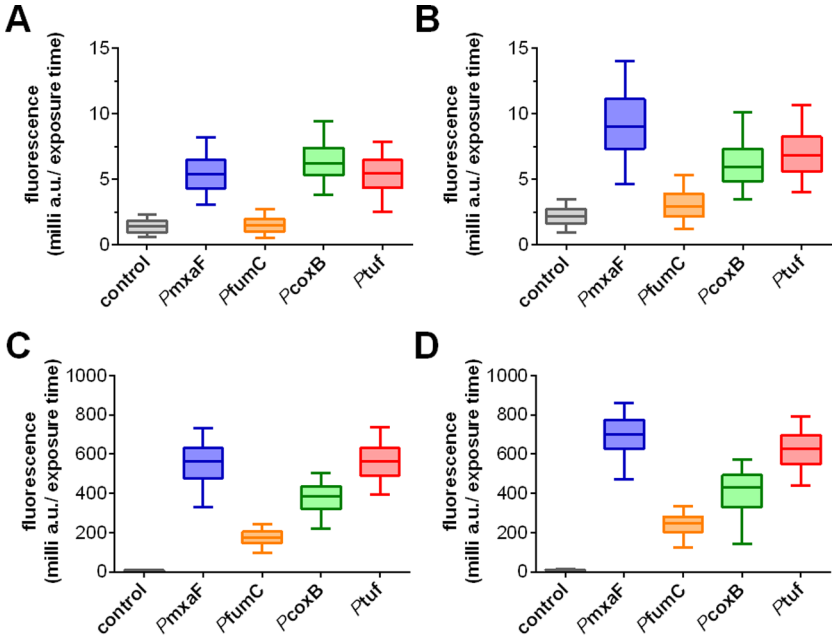

Figure 3. Single-cell fluorescence of *P*mxaF, *P*fumC, *P*coxB, and *P*tuf promoters as well as promoterless control constructs with either GFPmut3 (A, B) or mCherry (C, D) as the reporter during the mid-exponential growth phase of *M. extorquens* AM1. *M. extorquens* AM1 cells carrying pTE100-, pTE102-, pTE103-, pTE104-, and pTE105-GFPmut3 or -mCherry as reporter genes were cultivated in minimal medium with methanol (A, C) or succinate (B, D) as the sole carbon source. The fluorescence of a minimum of 400 individual cells at the mid-exponential growth phase was analyzed. Box, 25th to 75th percentile; horizontal line, median; upper and lower whiskers, 5th and 95th percentiles, respectively.

different growth stages of shaken liquid cultures on methanol or succinate medium (Figure 2). The single-cell fluorescence signals of the different constructs remained stable during all growth phases of all liquid cultures, indicating constitutive expression from the promoter independent of the cell's physiological status. Only in succinate grown cells did we notice a second, small nonfluorescent cell population emerging in the stationary phase (Figure 2, red bars). These cells could not be differentiated from the fluorescent cells in phase contrast images, so we hypothesize that they represent cells that died upon reaching the stationary phase. However, in mid-exponential phase, all cultures exhibited normally distributed fluorescence intensities on the single-cell level (Figure 2, dark blue bars), indicating the absence of population-based phenomena, such as bistability, for all constructs and growth media tested. Interestingly, fluorescence of cells grown on succinate showed a higher standard deviation than that of cells grown on methanol by approximately a factor of 2 (*P*mxaF, 2.5; *P*fumC, 2.2; *P*coxB, 1.6; *P*tuf, 1.9), indicating expression control that is slightly less tight in succinate medium.

Next, we analyzed fluorescence readouts from midexponential phase cultures in more detail. Measurements were repeated with all promoter−reporter constructs containing GFPmut3 or mCherry for comparison (Figure 3). Because no significant differences in growth rate (μ) were observed between the different strains (Table 1), the fluorescent readout served as a direct proxy for the intrinsic promoter activity of the different promoters. The expression pattern observed between both reporter systems was comparable (Figure 3) and followed the trend *P*fumC < *P*coxB < *P*tuf ≈ *P*mxaF. However, strains expressing mCherry constructs were more than 10 times brighter per millisecond exposure time than their GFPmut3 expressing analogues. In addition, the signal-to-noise level was much lower in mCherry expressing cells, and the fluorescence showed a much higher dynamic range, suggesting that mCherry

Table 1. Growth Rates of *M. extorquens* AM1 Carrying Different pTE Promoter−Reporter Constructs Grown in Minimal Medium Containing Methanol or Succinate[a]

strain	growth medium	growth rate (h^{-1})
M.ex. AM1 (pTE102-GFP)	Methanol	0.120 ± 0.026
M.ex. AM1 (pTE103-GFP)	Methanol	0.133 ± 0.025
M.ex. AM1 (pTE104-GFP)	Methanol	0.125 ± 0.019
M.ex. AM1 (pTE105-GFP)	Methanol	0.115 ± 0.031
M.ex. AM1 (pTE102-GFP)	Succinate	0.119 ± 0.031
M.ex. AM1 (pTE103-GFP)	Succinate	0.115 ± 0.036
M.ex. AM1 (pTE104-GFP)	Succinate	0.104 ± 0.019
M.ex. AM1 (pTE105-GFP)	Succinate	0.111 ± 0.020
M.ex. AM1 (pTE100-mChe)	Methanol	0.150 ± 0.019
M.ex. AM1 (pTE102-mChe)	Methanol	0.170 ± 0.002
M.ex. AM1 (pTE103-mChe)	Methanol	0.154 ± 0.018
M.ex. AM1 (pTE104-mChe)	Methanol	0.158 ± 0.013
M.ex. AM1 (pTE105-mChe)	Methanol	0.166 ± 0.063
M.ex. AM1 (pTE100-mChe)	Succinate	0.114 ± 0.030
M.ex. AM1 (pTE102-mChe)	Succinate	0.143 ± 0.014
M.ex. AM1 (pTE103-mChe)	Succinate	0.121 ± 0.014
M.ex. AM1 (pTE104-mChe)	Succinate	0.137 ± 0.006
M.ex. AM1 (pTE105-mChe)	Succinate	0.140 ± 0.036

[a]Given values are the average of at least two independent measurements ± SD. No significant differences were detected between all samples (one-way ANOVA, $p < 0.05$).

is better suited for accurate expression analysis in *M. extorquens* AM1 than is GFP. Compared to GFP, eYFP also showed an improved signal-to-noise ratio, better dynamic range, and stronger fluorescence signal, indicating that it also is suitable for expression analysis in *M. extorquens* AM1 (Supporting Information Figure S2). On the basis of these results, we propose the use of mCherry as the standard reporter protein for fluorescent readouts in *M. extorquens* AM1.

dx.doi.org/10.1021/sb500221v | *ACS Synth. Biol.* 2015, 4, 430−443

Table 2. Growth Rates of *M. extorquens* AM1 Δ*ccr* Strains Carrying Different pTE Promoter−Ccr Constructs Grown in Minimal Medium Containing Methanol or Succinate[a]

strain	growth medium	growth rate (h^{-1})	Ccr activity (mU/mg)
M. ex. AM1 (wild type)	Methanol	0.16 ± 0.01[64]	570 ± 80[75]
M.ex. AM1 Δ*ccr* (pTE100)	Methanol	[b]	[c]
M.ex. AM1 Δ*ccr* (pTE100-Ccr)	Methanol	0.07 ± 0.01	40 ± 0
M.ex. AM1 Δ*ccr* (pTE102-Ccr)	Methanol	0.15 ± 0.03	6400 ± 90
M.ex. AM1 Δ*ccr* (pTE103-Ccr)	Methanol	0.14 ± 0.02	390 ± 10
M.ex. AM1 Δ*ccr* (pTE104-Ccr)	Methanol	0.15 ± 0.02	2600 ± 110
M.ex. AM1 Δ*ccr* (pTE105-Ccr)	Methanol	0.13 ± 0.01	4400 ± 170
M. ex. AM1 (wild type)	Succinate	0.17 ± 0.01[64]	190 ± 20[75]
M.ex. AM1 Δ*ccr* (pTE100)	Succinate	0.16 ± 0.04	[c]
M.ex. AM1 Δ*ccr* (pTE100-Ccr)	Succinate	0.18 ± 0.05	70 ± 10
M.ex. AM1 Δ*ccr* (pTE102-Ccr)	Succinate	0.12 ± 0.02	5000 ± 270
M.ex. AM1 Δ*ccr* (pTE103-Ccr)	Succinate	0.15 ± 0.05	720 ± 10
M.ex. AM1 Δ*ccr* (pTE104-Ccr)	Succinate	0.12 ± 0.02	2600 ± 50
M.ex. AM1 Δ*ccr* (pTE105-Ccr)	Succinate	0.15 ± 0.04	4700 ± 130

[a]Given values are the averages of three independent measurements ± SD. [b]No growth. [c]Ccr activity could be determined.

Methylobrick Promoter-Driven Expression of Crotonyl-CoA Carboxylase/Reductase. In order to characterize promoter activities by a second, independent approach, the gene coding for crotonyl-CoA carboxylase/reductase (Ccr) from *M. extorquens* AM1 was chosen as the reporter. Ccr is the key enzyme of the ethylmalonyl-CoA pathway, the central pathway for biomass formation from C1 or C2 substrates, such as methanol or acetate, in *M. extorquens*.[39] The enzyme catalyzes the reductive carboxylation of crotonyl-CoA to ethylmalonyl-CoA. Deletion of *ccr* prohibits growth of *M. extorquens* AM1 on methanol (or other C1 and C2 substrates),[40] so methylotrophic growth of a *ccr* knockout is possible only when Ccr is complemented to sufficient levels (e.g., by plasmid-based expression).

To quantify promoter activities, we used the *ccr* knockout strain *M. extorquens* AM1 61ADH,[40] henceforth called *M. extorquens* AM1 Δ*ccr*, that was transformed with different promoter−*ccr* constructs in which the *ccr* gene was placed under the control of one of the four promoters. The growth rates of these *ccr*-complemented mutant strains were investigated in minimal medium containing methanol as the sole carbon source as well as in minimal medium containing succinate as a positive control. Expression of *ccr* under the control of any of the four promoters was sufficient to restore wild-type-like growth of *M. extorquens* AM1 Δ*ccr* on methanol (Table 2). In contrast, introduction of *ccr* in a promoterless plasmid resulted in slow growth of the *M. extorquens* AM1 Δ*ccr* mutant on methanol, demonstrating a very low background expression of *ccr* that rate limits the growth of this strain. This was confirmed by Ccr activity measurements in cell extracts of the different strains (Table 2). Ccr activities span 2 orders of magnitude, starting from promoterless constructs with approximately 1% relative activity and following the order *P*fumC (5−15%) < *P*coxB (40−50%) < *P*tuf (70−100%) ≈ *P*mxaF (100%). Notably, *P*coxB and *P*tuf showed very similar absolute expression levels on both carbon substrates, whereas *P*fumC was slightly upregulated on succinate, and *P*mxaF was slightly upregulated on methanol, as reported before.[41] In summary, these experiments independently confirmed the order of promoter strength obtained with mCherry as the reporter (Supporting Information Figure S3).

Expression Levels and Application of Polycistronic, Synthetic Operons. To investigate expression levels of synthetic operons and to test for positional effects of genes within operons, two vector constructs containing eYFP and mCherry in both possible permutations under the control of *P*coxB were generated. Single-cell eYFP and mCherry fluorescence was quantified after growth in liquid minimal medium (Supporting Information Figure S4). A negligible positional effect could be determined for mCherry fluorescence. mCherry appeared minimally brighter when upstream of eYFP (1.06-fold; two-tailed *t* test, $P = 0.044$). This effect was more pronounced for eYFP fluorescence when the eYFP gene was positioned upstream of the one encoding mCherry (1.4-fold; two-tailed *t* test, $P < 0.0001$), similar to other experiments in which some fluorescence reporter genes stimulate downstream gene expression to some extent.[42] In summary, our experiments did not indicate any substantial positional silencing effect, suggesting that the Methylobrick vector system is, in principle, suited to create polycistronic operons.

To demonstrate the applicability of polycistronic, synthetic operons *in vivo*, we sought to engineer *M. extorquens* AM1 for the production of value-added compounds from simple carbon substrates using the Methylobrick vector system. As mentioned earlier, the central pathway for biomass formation from methanol or acetate in *M. extorquens* is the ethylmalonyl-CoA pathway. This metabolic pathway features several CoA esters of C5 dicarboxylic acids that are of high interest for the chemical industry, which makes it a promising biotechnological source for the sustainable production of these C5 compounds.[43,44] However, the essential role of the ethylmalonyl-CoA pathway in C1 and C2 assimilation does not allow C5 building blocks to be depleted from *M. extorquens* AM1 by a simple pathway blockage because this would result in a complete breakdown of biomass formation, and thus survival, in this organism.[18] This is exemplified by the fact that the deletion of both isoforms of malyl-CoA/β-methylmalyl-CoA lyase (Δ*mclA1/A2*), the enzyme catalyzing the last step in the ethylmalonyl-CoA pathway, completely abolishes growth of *M. extorquens* AM1 on acetate (or other C1 and C2 carbon substrates).[45,46] To overcome this problem, we sought to equip *M. extorquens* AM1 Δ*mclA1/A2* with an additional pathway module that would allow the organism to form biomass from short-chain carbon substrates by alternative means.

For this purpose, we assembled a three-gene operon on the Methylobrick vector backbone that would allow the conversion

dx.doi.org/10.1021/sb500221v | *ACS Synth. Biol.* 2015, 4, 430−443

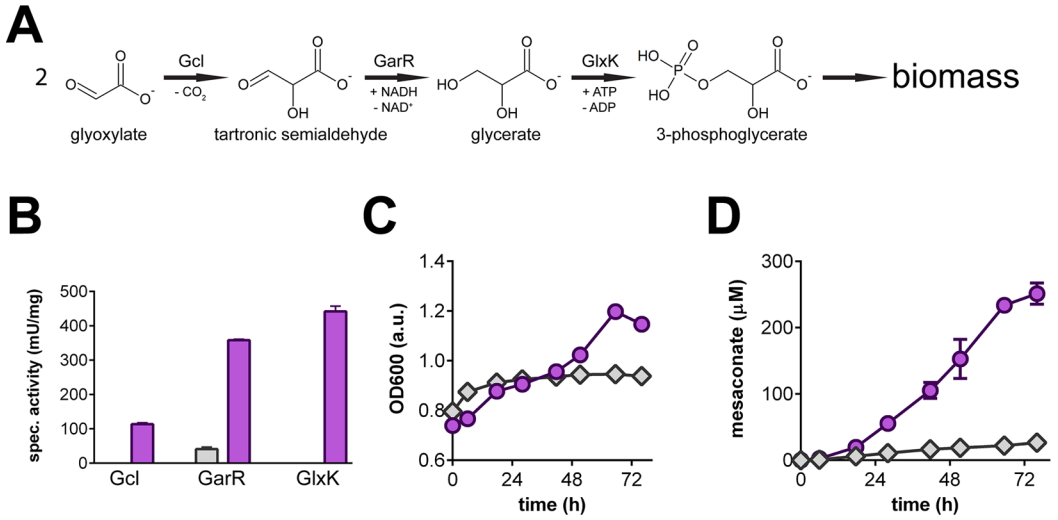

Figure 4. Engineering of a Δ*mclA1/A2* mutant strain of *M. extorquens* AM1 for mesaconate production from acetate and glyoxylate. (A) Three-enzyme glyoxylate fixation module introduced into the host that allows conversion of glyoxylate into 3-phosphoglycerate. (B) Quantification of enzyme activities in cell-free extracts of a Δ*mclA1/A2* mutant carrying the empty vector pTE102 (gray bars) or pTE102-Gly encoding the glyoxylate assimilation module (purple bars). The GarR activity in the negative control is due to some endogenous tartronic semialdehyde reductase activity of *M. extorquens* AM1. (C) Cultivation experiments on acetate and glyoxylate. Cells carrying pTE102 (gray diamonds) fail to grow, whereas cells carrying pTE102-Gly (purple circles) grow with an estimated doubling time of about 160 h. (D) Mesaconate production experiments on acetate and glyoxylate. Cells carrying pTE102 produce only negligible amounts of mesaconate (gray diamonds) compared to cells carrying pTE102-Gly that accumulate more than 10-fold the amount of mesaconate in the supernatant (purple circles). For panels B–D, representative experiments performed in triplicate are depicted (error bars indicate SD).

of the C2 compound glyoxylate into 3-phosphoglycerate, a central metabolite from which biomass can be generated. We reasoned that upon co-feeding of the C2 substrates acetate and glyoxylate, a *M. extorquens* AM1 Δ*mclA1/A2* mutant engineered with such a synthetic pathway module could survive and sustain biomass formation from glyoxylate (Figure 4A), whereas acetate could be converted into C5 dicarboxylic acids. When tested for functionality, all three enzyme activities of the synthetic operon could be quantified in cell extracts of a *M. extorquens* AM1 Δ*mclA1/A2* mutant complemented with the synthetic construct compared to that of the control, indicating that the pathway module for alternative biomass generation in *M. extorquens* was functional (Figure 4B).

Indeed, when a culture of *M. extorquens* AM1 Δ*mclA1/A2* that carried the empty Methylobrick vector pTE102 was incubated with acetate and glyoxylate, this noncomplemented mutant strain did not show any observable increase in OD_{600} and accumulated negligible amounts of the C5 compound mesaconate in the supernatant (Figure 4C,D). In contrast, *M. extorquens* AM1 Δ*mclA1/A2* × pTE102-Gly, carrying the synthetic glyoxylate pathway module, grew slowly when incubated under the same conditions with a doubling time of approximately 160 h, as calculated from the increase of OD_{600} over the time course of the experiment. More importantly, formation of mesaconate in the supernatant of the engineered strain was increased by more than an order of magnitude compared to that of the noncomplemented mutant. The maximum mesaconate concentration reached with this strain (32 mg L^{-1}) was comparable to a recently reported mesaconate production strain of *M. extorquens*. This production strain was based on partially depleting products from the ethylmalonyl-CoA pathway by overexpressing an unspecific CoA thioesterase and accumulated a maximum of 72 mg L^{-1} free mesaconate when cultivated on methanol medium.[44] However, in contrast to the latter, which showed a strong decrease in free mesaconate after maximum production by almost 50% to 42 mg L^{-1} within 16 h, the concentration of mesaconate in the supernatant of our strain remained stable for more than 30 h, indicating that our engineered strain shows a greater productivity tolerance. In summary, our experiments demonstrated that the Methylobrick vector system is well-suited to functionally express polycistronic operons in *M. extorquens* AM1 (e.g., for metabolic engineering purposes).

Genomic Integration and Expression of Methylobrick Constructs. To test the transfer of genetic constructs from Methylobrick vectors to the genome of *M. extorquens* AM1, we used a mini-Tn*5* delivery system that is based on the vector pAG408[47] and that is compatible with the flanking restriction sites of the Methylobrick vector MCS. This allows for the simple subcloning of genetic constructs from Methylobrick vectors and their subsequent delivery to the *Methylobacterium* genome. When tested with the mCherry reporter constructs, the integration of these constructs into the chromosome of *M. extorquens* AM1 via two-parental mating and mini-Tn*5* transposition appeared very effective, with fluorescent conjugants growing within 3 days. Under the fluorescence stereomicroscope, no obvious differences in fluorescence intensity were observed for most colonies of the same promoter–reporter construct. However, on the single-cell level, about 10% of the clones were significantly brighter than all other clones carrying the same inserts. This has been reported before[47] and is likely due to random insertions behind promoters that are more active than the inserted promoters or multiple insertions events in the same transconjugant.

Ten randomly chosen colonies for each promoter–reporter construct were picked and grown on minimal medium methanol to mid-exponential phase for single-cell characterization. Single-cell fluorescence was well visible, but it was approximately 1 order of magnitude lower with 13% relative fluorescence for *P*fumC, 11% for *P*coxB, and 8% for *P*tuf, as

dx.doi.org/10.1021/sb500221v | *ACS Synth. Biol.* 2015, 4, 430–443

compared to the plasmid-borne expression of mCherry. In summary, constitutive expression from single chromosomal insertions was driven from the Methylobrick promoters tested, following the order of promoter strength observed before (i.e., *P*fumC < *P*coxB ≈ *P*tuf; Figure 5). Thus, Tn5 delivery with pAG408 as a shuttle plasmid offers a fast and efficient approach for the integration and expression of single-copy Methylobrick modules in the *M. extorquens* AM1 chromosome.

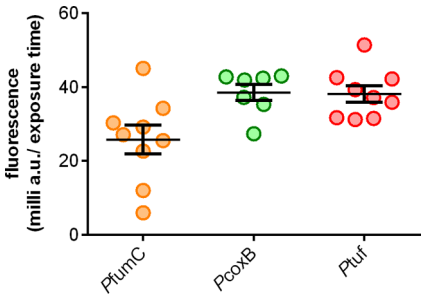

Figure 5. Single-cell fluorescence of independent insertions of *P*fumC, *P*coxB, and *P*tuf promoter constructs with mCherry as reporter into the genome of *M. extorquens* AM1. Each point represents the mean fluorescence of an independent clone carrying a chromosomal insertion of a *P*fumC-, *P*coxB-, or *P*tuf-mCherry construct that was delivered by Tn5 transposition. All clones were grown in methanol minimum medium until mid-exponential phase before the fluorescence was quantified for a minimum of 200 individual cells. The automated outlier detection method "Iterative Grubbs" of the software Prism 6 was used to remove unusually bright and dim transconjugants. Error bars depict the SEM.

Application of Brick Vectors and Tn5 Delivery in Other Alphaproteobacteria. To test the applicability of the Methylobrick vector system and the promoter library created in this study in other alphaproteobacterial model organisms, we introduced the plasmid-borne Methylobrick-mCherry constructs into three other species. These included *Agrobacterium tumefaciens* C58, *Caulobacter crescentus* CB15, and *Paracoccus denitrificans*, which represent the bio(techno)logically most relevant alphaproteobacterial orders *Rhizobiales*, *Caulobacterales*, and *Rhodobacterales*, respectively. When mCherry fluorescence was quantified on the single-cell level, the results demonstrated that all promoters were active in their alphaproteobacterial hosts, with *P*tuf consistently promoting the highest expression levels (Figure 6), whereas the other promoters showed similar patterns as that in *M. extorquens* AM1, with some exceptions in different hosts (e.g., *P*mxaF in *P. denitrificans*).

In addition to that, we also tested the Tn5-delivery and expression of reporter constructs in other alphaproteobacterial hosts. Matings were successful with *Sphingomonas melonis* Fr1, *Sphingomonas phyllosphaerae* DSM17258, *Sphingomonas wittichii* DSM6014, and *Bradyrhizobium japonicum* 110spc4 (H.-M. Fischer, R. Ledermann, personal communication). In all of these hosts we were able to detect significant mCherry fluorescence at the single-cell level, and even though we did not quantify the expression level exactly, the promoter *P*fumC proved to be the least active promoter in the tested heterologous hosts, whereas *P*coxB and *P*tuf yielded transconjugants of similar brightness, confirming the results obtained for *M. extorquens* AM1 (see above).

In summary, our results indicate the transferability of the promoters and vectors of the Methylobrick toolbox to other Alphaproteobacteria, which opens up new possibilities for detailed investigations and biotechnological applications in this diverse bacterial class.

CONCLUSIONS AND OUTLOOK

We have created a set of vectors that allow isocaudomeric cloning of genes and operons, whose expression is driven from one of four different promoters that allow constitutive expression of genes in *M. extorquens* AM1 at different levels. This Methylobrick system is compatible with other commonly employed expression vectors, allowing direct cloning of ORFs from the pET (Novagen) and pSEVA (http://seva.cnb.csic.es) systems. Furthermore, it offers stop codons in three reading frames, a RBS optimized for *Methylobacterium* and other Gram-negative bacteria, and a wide choice of restriction sites in the MCS.

Besides the previously described *P*mxaF promoter, we have characterized three novel promoters that all allow stable, constitutive gene expression in *M. extorquens* AM1 at different levels of expression. We have mapped the core elements of these promoters, allowing the use of these minimal promoter elements in future genetic constructs. Promoter activity was quantified by two independent approaches, yielding a definite order of the promoters on the two standard media used in *M. extorquens* AM1 cultivation.

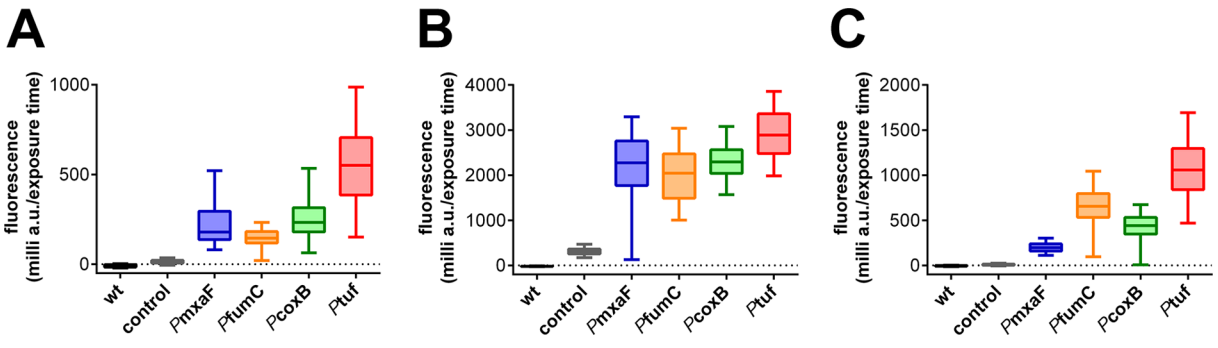

Figure 6. Single-cell fluorescence of *P*mxaF, *P*fumC, *P*coxB, and *P*tuf promoter as well as promoterless control constructs during mid-exponential growth phase of *Agrobacterium tumefaciens* C58 (A), *Caulobacter crescentus* CB15 (B), and *Paracoccus denitrificans* JVZ2585 (C). Cells of the three alphaproteobacterial species carrying pTE100-, pTE102-, pTE103-, pTE104-, and pTE105-mCherry and of the respective WT were cultivated in LB (A, C) or PYE (B) medium. The fluorescence of a minimum of 400 individual cells in midexponential growth phase was analyzed. Box, 25th to 75th percentile; horizontal line, median; upper and lower whiskers, 5th and 95th percentiles, respectively.

dx.doi.org/10.1021/sb500221v | *ACS Synth. Biol.* 2015, 4, 430−443

Table 3. Strains and Plasmids Used in This Study

strain or plasmid	genotype or relevant features[a]	source or ref
E. coli		
DH5α	supE44 ΔlacU169 (Φ80lacZDM15) hsdR17 recA1 endA1 gyrA96 thi-1 relA1	Life Technologies
S17-1λpir	recA, thi, pro, hsdR-M+RP4:2-Tc:Mu:Km Tn7 λpir; Tp^R, Sm^R	53
M. extorquens AM1		
M. extorquens AM1	wild-type	49
M. extorquens AM1 61ADH	Δ*ccr*; Km^R	40
M. extorquens AM1	Δ*mclA1/A2*; Km^R	45
Agrobacterium tumefaciens C58	wild-type	69
Caulobacter crescentus CB15	wild-type	70
Paracoccus denitrificans JVZ2585	Rif^R	51
Sphingomonas melonis Fr1	wild-type	71
Sphingomonas phyllosphaerae DSM17258	wild-type	72
Sphingomonas wittichii DSM6014	wild-type	73
Bradyrhizobium japonicum 110spc4	Spc^R	74
pCM80	*M. extorquens* AM1 expression vector, pCM62 derivative, *mxaF* promoter; Tc^R	20
pLM01	pCM80-based; Km^R	29
pTE100[b]	Brick vector, no promoter; Tc^R	this work
pTE101[c]	Brick vector, no promoter; Km^R	this work
pTE102	Brick vector, *mxaF* promoter; Tc^R	this work
pTE103	Brick vector, *fumC* promoter; Tc^R	this work
pTE104	Brick vector, *coxB* promoter; Tc^R	this work
pTE105	Brick vector, *tuf* promoter; Tc^R	this work
pTE100-GFP	Brick vector, no promoter, GFPmut3; Tc^R	this work
pTE100-mChe	Brick vector, no promoter, mCherry; Tc^R	this work
pTE100-eYFP	Brick vector, no promoter, eYFP; Tc^R	this work
pTE100-mChe-eYFP	Brick vector, no promoter, mCherry and eYFP; Tc^R	this work
pTE100-eYFP-mChe	Brick vector, no promoter, eYFP and mCherry; Tc^R	this work
pTE102-GFP	Brick vector, *mxaF* promoter, GFP; Tc^R	this work
pTE103-GFP	Brick vector, *fumC* promoter, GFP; Tc^R	this work
pTE104-GFP	Brick vector, *coxB* promoter, GFP; Tc^R	this work
pTE105-GFP	Brick vector, *tuf* promoter, GFP; Tc^R	this work
pTE102-mChe	Brick vector, *mxaF* promoter, mCherry; Tc^R	this work
pTE103-mChe	Brick vector, *fumC* promoter, mCherry; Tc^R	this work
pTE104-mChe	Brick vector, *coxB* promoter, mCherry; Tc^R	this work
pTE105-mChe	Brick vector, *tuf* promoter, mCherry; Tc^R	this work
pTE102-mChe-eYFP	Brick vector, *mxaF* promoter, mCherry and eYFP; Tc^R	this work
pTE103-mChe-eYFP	Brick vector, *fumC* promoter, mCherry and eYFP; Tc^R	this work
pTE104-mChe-eYFP	Brick vector, *coxB* promoter, mCherry and eYFP; Tc^R	this work
pTE105-mChe-eYFP	Brick vector, *tuf* promoter, mCherry and eYFP; Tc^R	this work
pTE102-eYFP-mChe	Brick vector, *mxaF* promoter, eYFP and mCherry; Tc^R	this work
pTE103-eYFP-mChe	Brick vector, *fumC* promoter, eYFP and mCherry; Tc^R	this work
pTE104-eYFP-mChe	Brick vector, *coxB* promoter, eYFP and mCherry; Tc^R	this work
pTE105-eYFP-mChe	Brick vector, *tuf* promoter, eYFP and mCherry; Tc^R	this work
pTE100-Ccr	Brick vector, *ccr*; Tc^R	this work
pTE102-Ccr	Brick vector, *mxaF* promoter, *ccr*; Tc^R	this work
pTE103-Ccr	Brick vector, *fumC* promoter, *ccr*; Tc^R	this work
pTE104-Ccr	Brick vector, *coxB* promoter, *ccr*; Tc^R	this work
pTE105-Ccr	Brick vector, *tuf* promoter, *ccr*; Tc^R	this work
pTE102-Gly	Brick vector, *mxaF* promoter, *gcl*, *garR*, *glxK*; Tc^R	this work
pJBA28	Mini-Tn5 delivery vector, $P_{A1/04/03}$ GFPmut3, R6K-ori; Amp^R, Tc^R	57
pMP7604	Cloning vector, $P_{A1/04/03}$ mCherry, Tc^R	58
pAG408	Mini-Tn5 delivery vector, no promoter, GFP, R6K-ori; Amp^R, Km^R, Gm^R	47
pMRE-103-mCherry	Mini-Tn5 delivery vector, *fumC* promoter mCherry; Gm^R, Amp^R	this work
pMRE-104-mCherry	Mini-Tn5 delivery vector, *coxB* promoter mCherry; Gm^R, Amp^R	this work
pMRE-105-mCherry	Mini-Tn5 delivery vector, *tuf* promoter mCherry; Gm^R, Amp^R	this work

[a] Tp^R, trimethoprim resistance; Sm^R, streptomycin resistance; Km^R, kanamycin resistance; Rif^R, rifampicin resistance; Spc^R, spectinomycin resistance; Tc^R, tetracycline resistance [b] Compared to pCM62, the backbone of pTE100 carries two point mutations, G3610A and T5307G. Neither mutation interferes with plasmid function. [c] Compared to pCM62, the backbone of pTE101 backbone carries one point mutation, G3642A. The mutation does not interfere with plasmid function.

dx.doi.org/10.1021/sb500221v | ACS Synth. Biol. 2015, 4, 430−443

Table 4. Primers Used in the Study[a]

target	name	sequence	restriction site
GFPmut3	GFPmut3_fw1	5′-CGGGCC**ATTAAT**GCATGCGTAAAG-3′	AseI
GFPmut3	GFPmut3_rev1	5′-CCCGCC**GGATCC**CTTATTTGTATAGTTC-3′	BamHI
mCherry	mCherry_fw1	5′-GACACGC**CATATG**GTGAGCAAG-3′	NdeI
mCherry	mCherry_rev1	5′-GCGCCTCG**GAATTC**CTTGTACAG-3′	EcoRI
eYFP	eYFP_fw1	5′-CCTCGCAGC**CATATG**CTGAGCAAGG-3′	NdeI
eYFP	eYFP_rev1	5′-CCGC**GAATTC**ATTACTTGTACAGCTCGTCC-3′	EcoRI
*P*tuf	tuf_fw1	5′-GACGT**TCTAGA**TGCTGGTGCGGGTGCTC-3′	XbaI
*P*tuf	tuf_rev1	5′-CAAGGCC**AAGCTT**CGTGCAATCCTACCG-3′	HindIII
*P*coxB	pcoxB_fw1	5′-CCTGCAT**TCTAGA**CCGTATCCCCAGAG-3′	XbaI
*P*coxB	pcoxB_rev1	5′-CGTTCGC**AAGCTT**ATGTCCCCGCTTGG-3′	HindIII
fumC	RACE_fumC_1	5′-CAGCAGCCGCTCCTGAACCTC-3′	
fumC	RACE_fumC_2	5′-GCGGTTGCAATGATCGTTGGG-3′	
fumC	RACE_fumC_3	5′-GTTGGCGTTCATGTTGGACTG-3′	
coxB	RACE_coxB_1	5′-CCACCGCCACGAGGATCAGGAC-3′	
coxB	RACE_coxB_2	5′-CGATCGCCGTGTTGTGCGTGG-3′	
coxB	RACE_coxB_3	5′-CCGAGATCGCGAAGGCGATCC-3′	
tuf	RACE_tuf_1	5′-GACGGCTTCCTTGCCGATCTTG-3′	
tuf	RACE_tuf_2	5′-GCCCTTGGTGATCGGGATGTC-3′	
tuf	RACE_tuf_3	5′-CAGGATCGCGCCGTCCATCTG-3′	
gcl	Gibson_gcl_fw	5′-GACCATGATTACGCCAAGCTTAGATCTTGATGGAATTCTGTACATCTAGAAATAAG-3′	
gcl	Gibson_gcl_rv	5′-ATGATCACAATAGCATTATTCATAGTGCATGAAGC-3′	
garR	Gibson_garR_fw	5′-ATGCACTATGAATAATGCTATTGTGATCATCTAGAAATAAG-3′	
garR	Gibson_garR_rv	5′-ATGTTCAGTATGCGATTAACGAGTAACTTCGACTTTC-3′	
glxK	Gibson_glxK_fw	5′-GAAGTTACTCGTTAATCGCATACTGAACATCTAGAAATAAG-3′	
glxK	Gibson_glxK_rv	5′-CGACGGCCAGTGAATTAGGTACCTGCAGGATTAGTTCTTAATTCCCTGACC-3′	

[a]Nucleotides in bold and underlined are recognition sites for endonuclease restriction enzymes.

To standardize the characterization of genetic elements in the Methylobrick system, we propose to quantify reporter-based fluorescence at the single-cell level relative to the standard promoter *P*mxaF, using mCherry as the fluorescence reporter, which is superior compared to GFPmut3 in *M. extorquens* AM1. The general availability of fluorescence microscopes enables the convenient characterization of these genetic elements and provides additional information on their behavior in cell populations, thereby allowing the quantification of expression variability and/or the detection of possible population-based phenomena (e.g., bistability). We estimate that for an experienced user image acquisition and image analysis to characterize one promoter takes about 40 min.

On the basis of the broad host range vector pCM80,[20] the here-introduced Methylobrick vectors and the standard set of Methylobrick promoters are functional in many different alphaproteobacterial hosts, which enhances the molecular toolbox for this group of organisms and enables further genetic, biotechnological, and environmental studies. We also demonstrated that genes integrated into the host chromosome under the control of the newly characterized set of promoters are actively and stably transcribed in a number of Alphaproteobacteria, so that chromosomal integration of Methylobrick modules by Tn5 transposon delivery offers a quick and easy method for introducing heterologous genetic elements into alphaproteobacterial species that either do not allow stable maintenance of plasmids or for which a continuous antibiotic selection is not possible (e.g., *Bradyrhizobium japonicum*, an important model organism for nitrogen fixation in root nodules).

In summary, the applicability of the described Methylobrick vectors in a variety of Alphaproteobacteria enhances the toolbox for this metabolically diverse and biotechnologically relevant class of bacteria. Future adaptions of the Methylobrick system might include the integration of the Cre−Lox system for the targeted delivery of constructs to *M. extorquens* AM1[48] as well as the addition of more genetic elements, such as different RBS modules or more promoters, to further enhance the tunability of synthetic operons in *M. extorquens* and other Alphaproteobacteria. Methylobrick plasmids pTE100 to pTE105 have been made available to the community through the Addgene plasmid repository (www.addgene.org).

MATERIALS AND METHODS

Bacterial Strains, Culture Conditions, and Plasmid Delivery. If not mentioned otherwise, wild-type (WT) *M. extorquens* AM1[49] was used. For Ccr complementation assays, the Δ*ccr* mutant *M. extorquens* AM1 61ADH was used.[40] For the overproduction of mesaconate, the Δ*mclA1/A2* mutant of *M. extorquens* AM1 was used.[45] *E. coli* DH5α was used for construction and amplification of all plasmids used in this work. *M. extorquens* AM1 was cultured at 28 °C in minimal medium,[50] supplemented with either 123.6 mM methanol, 30.8 mM succinate, or 10 mM acetate as well as 10 mM glyoxylate, or in Nutrient Broth (NB) without additional NaCl (Sigma-Aldrich, St. Louis, MO, USA). *E. coli* DH5α was cultured in LB medium at 37 °C. When appropriate, media were supplemented with tetracycline, kanamycin, or gentamycin at a concentration of 10, 50, or 20 μg mL^{-1}, respectively. For growth experiments, at least two independent cultures were inoculated at an initial OD_{600} of 0.05 and cultured in baffled shake flasks at 28 °C. Growth rates were determined from exponential fits of OD_{600}-based growth curves using GraphPad Prism 6 software.

Sphingomonas melonis Fr1, *Sphingomonas phyllosphaerae* DSM17258, *Sphingomonas wittichii* DSM6014, *Bradyrhizobium*

japonicum 110spc4, *Caulobacter crescentus* CB15, and *Agrobacterium tumefaciens* C58 were laboratory stocks. *Paracoccus denitrificans* JVZ2585 is a spontaneous rifampicin-resistant derivative of *P. denitrificans* DSM413 obtained by selection with 50 μg mL^{-1} rifampicin.[51] These strains were grown at 28 °C on solidified medium (1.5% agar) or as 30 mL cultures in 100 mL baffled flasks (with shaking at 200 rpm) in LB medium (*P. denitrificans* and *A. tumefaciens*), NB medium (all *Sphingomonas* species), PSY medium[52] (*B. japonicum*), or PYE medium (0.2% peptone, 0.1% yeast extract, 0.02% $MgSO_4 \cdot 7H_2O$, 0.01% $CaCl_2 \cdot H_2O$; *C. crescentus*). Tetracycline to maintain plasmids was added to the media in the following concentrations (μg mL^{-1}): 2 (*C. crescentus*), 5 (*A. tumefaciens*), and 0.5 (*P. denitrificans*). For *A. tumefaciens* and *C. crescentus*, electroporation was performed on a GenePulser Xcell system (Bio-Rad) using the standard preset *E. coli* program. For *P. denitrificans*, plasmids were delivered by conjugal transfer from *E. coli* S17-1λpir[53] with mating on minimal medium without a carbon source as previously described.[54] Mating mixtures were diluted and plated on LB agar plates containing tetracycline (0.5 μg mL^{-1}) and rifampicin (50 μg mL^{-1}) for plasmid selection and counterselection of *E. coli*. Transconjugants were reliably obtained from 10-fold dilutions of the mating mixtures.

Plasmid Construction. All plasmids used and created in this study are presented in Table 3. All oligonucleotides are listed in Table 4. Cloning was performed according to standard protocols.[55] Restriction enzymes and T4 DNA ligase were obtained from NEB/Bioconcept (Allschwil, Switzerland). PCRs were conducted with Phusion polymerase (Thermo Scientific, Wohlen, Switzerland) following the recommendations of the manufacturer using the protocol for GC-rich templates; in short, 10 μL of Phusion 5× GC buffer, 5 μL 2 mM dNTPs, 12.5 μL each of 2 μM forward and reverse primers, 0.5 μL Phusion polymerase, up to 2.5 μL DMSO, 100 ng of template DNA, and water (to 50 μL total volume). Initial denaturation was performed at 98 °C for 5 min, followed by 35 cycles of 98 °C for 20 s, 55 °C for 30 s, 72 °C for 30−60 s (60 s per 1 kb), and a final extension at 72 °C for 5 min. Correct plasmid sequences were verified by Sanger sequencing (Microsynth, Balgach, Switzerland). Electroporation was used for plasmid delivery into *M. extorquens* AM1 as described previously.[56]

The Methylobrick MCS was created by annealing a 1:1 mixture of oligonucleotide "lead" (5′-CAT GGA ATT CTG TAC ATC TAG AAA TAA GAA GGA GAT ATA ATT AAT CCA TGG CAA TTG AAG CTT AGA TCT TGA CTA GTC CTG CAG GTA CC-3′) and "lag" (5′-GAA TTC TGT ACA TCT AGA AAT AAG AAG GAG ATA TAA TTA ATC CAT GGC AAT TGA AGC TTA GAT CTT GAC TAG TCC TGC AGG TAC CTA ATT-3′) by heating the mixture to 95 °C for 3 min and slowly cooling the mix to 25 °C within 3 h. This created an insert with overhanging ends that was ligated into an EcoRI and PciI digested pCM80 backbone[20] to create pTE100 and into a similarly digested pLM01 to create pTE101, respectively.

Promoter modules were created as described in the following. pTE102 was created by excising *P*mxaF from pCM80 with VspI and HindIII and ligation into the VspI and HindIII digested, dephosphorylated pTE100 backbone. pTE103 was created by digesting a synthesized DNA fragment (Eurofins MWG Operon, Ebersberg, Germany) containing *P*fumC with XbaI and HindIII and ligating this fragment in the similarly digested pTE100 backbone. pTE104 and pTE105 were created by amplifying the promoter fragments of *P*coxB and *P*tuf from genomic *M. extorquens* AM1 DNA using primer pairs PcoxB_fw1(XbaI) and PcoxB_rev1(HindIII) and tuf_fw1(XbaI) and tuf_rev1(HindIII), respectively. The PCR fragments were digested with XbaI and HindIII and subsequently cloned into the XbaI and HindIII digested pTE100 backbone. Promoter sequences contained in these plasmids can be found in Supporting Information Figure 1.

Reporter modules were created as follows. All fluorescent protein genes were amplified via PCR. GFPmut3 was amplified from pJBA28[57] using GFPmut3_fw1 and GFPmut3_rev1 containing restriction sites for AseI and BamHI, respectively; mCherry was amplified from pMP7604[58] using mCherry_fw1 and mCherry_rev1 containing restriction sites for NdeI and EcoRI, respectively; eYFP was amplified from pUC18T-mini-Tn7T-Gm-eyfp[37] using eYFP_fw1 and eYFP_rev1 containing restriction sites for NdeI and EcoRI, respectively. PCR fragments were digested with AseI and HindIII or NdeI and EcoRI and cloned into the correspondingly digested pTE100 backbones. A DNA fragment coding for *M. extorquens* AM1 *ccr* was excised from pGS6[59] by digestion with NdeI and HindIII and cloned into pTE100 digested with AseI and HindIII.

Thereafter, isocaudomeric cloning (as explained in Figure 1) was used to combine promoter and reporter modules to yield functional reporter constructs and synthetic operons. To create mini-Tn5 transposon-based delivery vectors, pTE103-mCherry, pTE104-mCherry, and pTE105-mCherry were used as donors and digested with EcoRI and KpnI to excise the promoter−reporter insert that was ligated into the EcoRI and KpnI digested pAG408 vector.[47] This resulted in pMRE-mini-Tn5-promotor-fluorescent protein delivery vectors that confer ampicillin resistance and a transposable gentamycin resistance. *E. coli* S17-λpir was transformed with these constructs and served as donor strain for two-parental mating.

Due to time constraints, plasmid pTE102-Gly containing the glyoxylate assimilation module was created according to the Gibson method,[60] mimicking the assembly by stepwise isocaudomeric cloning. To this end, the genes encoding for Gcl, GarR, and GlxK were amplified from *E. coli* K-12 MG1655 genomic DNA with primers for Gibson assembly (see Table 4). The vector pTE102 was digested with SpeI and used as backbone in the assembly reaction.

Two-Parental Mating for Mini-Tn5 Transposon Delivery. Tn5-delivery was performed by two-parental mating. To that end, overnight cultures of *E. coli* S17-λpir carrying the respective pMRE-mini-Tn5 delivery plasmids and *M. extorquens* AM1 WT were harvested by centrifugation for 15 min at 7000*g* and washed in NB twice before cells were resuspended in NB. Equivalent amounts of cells of both strains were mixed, spun once more, and resuspended in NB to a final OD_{600} between 10 and 20. 100 μL droplets of these mixtures were pipetted onto NB plates containing no antibiotics, and the plates were incubated overnight at 28 °C. Cells were recovered from the mating plates using 1 mL 10 mM $MgCl_2$, and dilution series of the recovered cells were plated onto minimal medium containing gentamycin and methanol for selection of Tn5 insertion events and counterselection of *E. coli*.

Fluorescence Microscopy and Image Analysis. Bacterial cells collected from liquid cultures were fixed in 4% paraformaldehyde as described elsewhere.[61] Briefly, bacteria were harvested by centrifugation at 12 000*g* for 2 min, washed once with 1× PBS, and resuspended in one volume of 1× PBS. Subsequently, three volumes of PBS-buffered 4% paraformaldehyde were added to the cells and were incubated at room

temperature for 3 h. To remove paraformaldehyde again, cells were washed twice with 1× PBS before they were resuspended in one volume of 1× PBS. To allow long-term storage, one volume of 100% ethanol was added before the cells were stored at −20 °C in the dark. Microscopy was performed using an AxioObserver D1 (Carl Zeiss GmbH, Oberkochen, Germany) with attached light source X-Cite 120Q (Lumen Dynamics Group Inc., Mississauga, Canada). GFPmut3 and eYFP emission was visualized using Zeiss filterset 38 HE (BP 470/40 nm/FT 495 nm/BP 525/50 nm), and mCherry was visualized using Zeiss filterset 43 HE (BP 550/25 nm/FT 570 nm/BP 605/70 nm). Samples were spotted on gelatin-treated 10-well Teflon-coated slides (Tekdon, Myakka City, FL, USA) in appropriate dilutions and were mounted using Citifluor AF1 antifade mounting resin (Citifluor Ltd., London, UK). Samples were observed with a Zeiss 100× EC Plan-Neofluar oil objective (1.3 NA, Phaco 3). Multichanneled fluorescence and phase contrast images were acquired using an AxioCam Mrm camera (Carl Zeiss GmbH) and the program AxioVision 4.8 (Carl Zeiss GmbH). For the observation of colonies, an epifluorescence stereomicroscope Discovery.V8 (Carl Zeiss GmbH), equipped with Zeiss filterset 38 HE for green fluorescence emitting fluorophores and Zeiss filterset 14 for red fluorescence emitting fluorophores, was used. For image analysis, images were imported into the software Fiji as 8 bit images.[62] If necessary, phase shifts between phase contrast and fluorescence channels were performed before the phase contrast channel was used to create a reference mask of all bacterial cells per image in the phase contrast channel. The reference mask was transferred to the corresponding fluorescence channel(s), and average gray intensity of individual cells was determined. Background fluorescence was determined for every individual image and was subtracted from the determined mean gray intensity. Finally, data was normalized against exposure time to allow comparability between different fluorophores and microscopy settings.

5′ Rapid Amplification of cDNA Ends (5′ RACE). Total RNA of *M. extorquens* AM1 was purified using the RNeasy mini kit (Qiagen) according to the manufacturer's instructions. Total RNA was treated with DNase I (Qiagen) prior to cDNA synthesis. cDNA synthesis and subsequent PCRs were performed using the 5′/3′ RACE kit (second generation; Roche) according to the manufacturer's instructions and as described previously.[63] The primers RACE_fumC/coxB/tuf_1 were used for cDNA amplification, and primers RACE_fumC/coxB/tuf_2 and RACE_fumC/coxB/tuf_3 were used for subsequent nested PCRs (for primer sequences, see Table 4). PCR products were gel-purified, TOPO-cloned using the TOPO TA cloning kit (Life Technologies) according to the manufacturer's instructions, and sequenced (Microsynth).

Preparation of Cell Extracts and Enzyme Activity Assays of Ccr, Gcl, GarR, and GlxK. *M. extorquens* AM1 WT and 61ADH transformed with the respective plasmids were grown on minimal medium[64] supplemented with succinate or methanol and tetracycline. Exponential-phase cultures were harvested by centrifugation, resuspended in 100 mM Tris-HCl buffer, pH 7.8, and lysed by sonication. The crude cell extract was centrifuged for 1 h at 20 000*g* to clear the lysate. Enzyme assays were carried out on a Cary-60 UV/Vis spectrophotometer (Agilent) at 30 °C using quartz cuvettes (3 or 10 mm i.d.; Hellma). Activity of Ccr in the supernatant fraction of the lysate was assayed spectrophotometrically as described previously.[39]

M. extorquens AM1 Δ*mclA1/A2* transformed with the plasmids pTE102 or pTE102-Gly was grown on minimal medium supplemented with acetate, glyoxylate, tetracycline, and kanamycin. Harvest and preparation of the cell extracts were carried out in the same way as described for Ccr assays. Activities of Gcl and GarR were assayed in a modified coupled spectrophotometric assay.[65] In short, a reaction mixture of 0.2 mL contained 50 mM phosphate buffer, pH 7.5, 1 mM $MgCl_2$, 0.1 mM thiamine diphosphate, 0.2 mM NADH, and cell extract containing 20 μg of total protein. The reaction was started by addition of 2 mM glyoxylate, and the oxidation of NADH was followed at 340 nm. Gcl and GarR activities were assayed with addition of excess purified GarR and Gcl, respectively.

Activity of GlxK was assayed in a modified coupled spectrophotometric assay with pyruvate kinase.[66] In short, a reaction mixture of 0.2 mL contained 50 mM phosphate buffer, pH 7.5, 10 mM $MgCl_2$, 0.5 mM ATP, 2.5 mM PEP, 3 mM phenylhydrazine hydrochloride, 1 U purified pyruvate kinase (Sigma-Aldrich), and cell extract containing 5 μg of total protein. The reaction was started by addition of 0.5 mM glycerate, and the formation of the phenylhydrazone derivative of pyruvate was followed at 312 nm.

The protein content of the cell extracts was determined by the Bradford method,[67] using BSA as a standard.

Quantification of Organic Acids. Quantification of organic acids was performed as described previously.[68] In brief, succinic acid was added to the cell-free supernatant of growing cultures as an internal standard, and organic acids were separated using a Phenomenex Rezex ROA organic acid H+ (8%, 300 × 7.8 mm) column connected to a Waters Alliance 2690 HPLC system.

■ ASSOCIATED CONTENT

Ⓢ Supporting Information

Analysis of the different promoter regions (S1), dynamic range and background to signal ratio for the different fluorescence reporters (S2), comparison of mCherry fluorescence and Ccr activity as reporter (S3), and polycistronic permutation analysis (S4). This material is available free of charge via the Internet at http://pubs.acs.org.

■ AUTHOR INFORMATION

Corresponding Author

*Phone: +41-44-6323654. E-mail: toerb@ethz.ch.

Present Address

‡Laboratory of Biomaterials, Eidgenössische Materialprüfanstalt (Empa), Lerchenfeldstrasse 5, 9014 St. Gallen, Switzerland.

Author Contributions

†These authors contributed equally to this work. L.S.v.B., M.R.E., J.A.V., and T.J.E. designed the research; L.S.v.B., M.R.E., and R.W. performed the experiments; L.S.v.B., M.R.E., R.W., J.A.V., and T.J.E. analyzed or provided data; and L.S.v.B., M.R.E., and T.J.E. wrote the manuscript.

Notes

The authors declare no competing financial interest.

■ ACKNOWLEDGMENTS

We thank Anne Francez-Charlot for sharing unpublished RNA-Seq data, Raoul Rosenthal for kindly providing crotonyl-CoA, Cedric Bergande and Aron Gagliardi for creating *M. extorquens* AM1 chromosomal insertion strains by Tn5 delivery during the Blockkurs, and Raphael Ledermann for testing Tn5 delivery to

B. japonicum. This work was supported by the Ambizione program of the Swiss National Science Foundation (SNF research grant PZ00P3_136828/1) and by an ETH grant (ETH-41 12-2) to T.J.E.

REFERENCES

(1) Elowitz, M., and Lim, W. A. (2010) Build life to understand it. *Nature 468*, 889−890.
(2) Benner, S. A., and Sismour, A. M. (2005) Synthetic biology. *Nat. Rev. Genet. 6*, 533−543.
(3) Gibson, D. G., Glass, J. I., Lartigue, C., Noskov, V. N., Chuang, R. Y., Algire, M. A., Benders, G. A., Montague, M. G., Ma, L., Moodie, M. M., Merryman, C., Vashee, S., Krishnakumar, R., Assad-Garcia, N., Andrews-Pfannkoch, C., Denisova, E. A., Young, L., Qi, Z. Q., Segall-Shapiro, T. H., Calvey, C. H., Parmar, P. P., Hutchison, C. A., 3rd, Smith, H. O., and Venter, J. C. (2010) Creation of a bacterial cell controlled by a chemically synthesized genome. *Science 329*, 52−56.
(4) Knight, T. Draft standard for BioBrick biological parts. *OpenWetWare*, 2007, http://hdl.handle.net/1721.1/45138.
(5) Aleksic, J., Bizzari, F., Cai, Y., Davidson, B., de Mora, K., Ivakhno, S., Seshasayee, S., Nicholson, J., Wilson, J., Elfick, A., French, C., Kozma-Bognar, L., Ma, H., and Millar, A. (2007) Development of a novel biosensor for the detection of arsenic in drinking water. *IET Synth. Biol. 1*, 87−90.
(6) Harger, M., Zheng, L., Moon, A., Ager, C., An, J. H., Choe, C., Lai, Y. L., Mo, B., Zong, D., Smith, M. D., Egbert, R. G., Mills, J. H., Baker, D., Pultz, I. S., and Siegel, J. B. (2013) Expanding the product profile of a microbial alkane biosynthetic pathway. *ACS Synth. Biol. 2*, 59−62.
(7) Chen, S., Zhang, H., Shi, H., Ji, W., Feng, J., Gong, Y., Yang, Z., and Ouyang, Q. (2012) Automated design of genetic toggle switches with predetermined bistability. *ACS Synth. Biol. 1*, 284−290.
(8) Kang, M.-K., Lee, J., Um, Y., Lee, T. S., Bott, M., Park, S. J., and Woo, H. M. (2014) Synthetic biology platform of CoryneBrick vectors for gene expression in *Corynebacterium glutamicum* and its application to xylose utilization. *Appl. Microbiol. Biotechnol. 98*, 5991−6002.
(9) Radeck, J., Kraft, K., Bartels, J., Cikovic, T., Durr, F., Emenegger, J., Kelterborn, S., Sauer, C., Fritz, G., Gebhard, S., and Mascher, T. (2013) The *Bacillus* BioBrick Box: generation and evaluation of essential genetic building blocks for standardized work with *Bacillus subtilis*. *J. Biol. Eng. 7*, 29.
(10) Boyle, P. M., Burrill, D. R., Inniss, M. C., Agapakis, C. M., Deardon, A., Dewerd, J. G., Gedeon, M. A., Quinn, J. Y., Paull, M. L., Raman, A. M., Theilmann, M. R., Wang, L., Winn, J. C., Medvedik, O., Schellenberg, K., Haynes, K. A., Viel, A., Brenner, T. J., Church, G. M., Shah, J. V., and Silver, P. A. (2012) A BioBrick compatible strategy for genetic modification of plants. *J. Biol. Eng. 6*, 8.
(11) Olah, G. A. (2013) Towards oil independence through renewable methanol chemistry. *Angew. Chem., Int. Ed. 52*, 104−107.
(12) MacLennan, D. G., Gow, J. S., and Stringer, D. A. (1973) Methanol: Bacterium process for SCP. *Process Biochem. 8*, 22−24.
(13) Anthony, C. (1982) *The Biochemistry of Methylotrophs*, Academic Press, London, United Kingdom.
(14) Schrader, J., Schilling, M., Holtmann, D., Sell, D., Filho, M. V., Marx, A., and Vorholt, J. A. (2009) Methanol-based industrial biotechnology: current status and future perspectives of methylotrophic bacteria. *Trends Biotechnol. 27*, 107−115.
(15) Marx, C. J., Bringel, F., Chistoserdova, L., aMoulin, L., Farhan Ul Haque, M., Fleischman, D. E., Gruffaz, C., Jourand, P., Knief, C., Lee, M. C., Muller, E. E., Nadalig, T., Peyraud, R., Roselli, S., Russ, L., Goodwin, L. A., Ivanova, N., Kyrpides, N., Lajus, A., Land, M. L., Medigue, C., Mikhailova, N., Nolan, M., Woyke, T., Stolyar, S., Vorholt, J. A., and Vuilleumier, S. (2012) Complete genome sequences of six strains of the genus *Methylobacterium*. *J. Bacteriol. 194*, 4746−4748.
(16) Vuilleumier, S., Chistoserdova, L., Lee, M. C., Bringel, F., Lajus, A., Zhou, Y., Gourion, B., Barbe, V., Chang, J., Cruveiller, S., Dossat, C., Gillett, W., Gruffaz, C., Haugen, E., Hourcade, E., Levy, R., Mangenot, S., Muller, E., Nadalig, T., Pagni, M., Penny, C., Peyraud, R., Robinson, D. G., Roche, D., Rouy, Z., Saenampechek, C., Salvignol, G., Vallenet, D., Wu, Z., Marx, C. J., Vorholt, J. A., Olson, M. V., Kaul, R., Weissenbach, J., Medigue, C., and Lidstrom, M. E. (2009) *Methylobacterium* genome sequences: a reference blueprint to investigate microbial metabolism of C1 compounds from natural and industrial sources. *PLoS One 4*, e5584.
(17) Gan, H. M., Chew, T. H., Hudson, A. O., and Savka, M. A. (2012) Genome sequence of *Methylobacterium* sp strain GXF4, a xylem-associated bacterium isolated from *Vitis vinifera* L. grapevine. *J. Bacteriol. 194*, 5157−5158.
(18) Peyraud, R., Schneider, K., Kiefer, P., Massou, S., Vorholt, J. A., and Portais, J. C. (2011) Genome-scale reconstruction and system level investigation of the metabolic network of *Methylobacterium extorquens* AM1. *BMC Syst. Biol. 5*, 189.
(19) Marx, C. J., and Lidstrom, M. E. (2004) Development of an insertional expression vector system for *Methylobacterium extorquens* AM1 and generation of null mutants lacking mtdA and/or fch. *Microbiology 150*, 9−19.
(20) Marx, C. J., and Lidstrom, M. E. (2001) Development of improved versatile broad-host-range vectors for use in methylotrophs and other Gram-negative bacteria. *Microbiology 147*, 2065−2075.
(21) Choi, Y. J., Bourque, D., Morel, L., Groleau, D., and Míguez, C. B. (2006) Multicopy integration and expression of heterologous genes in *Methylobacterium extorquens* ATCC 55366. *Appl. Environ. Microbiol. 72*, 753−759.
(22) Gutiérrez, J., Bourque, D., Criado, R., Choi, Y. J., Cintas, L. M., Hernández, P. E., and Míguez, C. B. (2005) Heterologous extracellular production of enterocin P from *Enterococcus faecium* P13 in the methylotrophic bacterium *Methylobacterium extorquens*. *FEMS Microbiol. Lett. 248*, 125−131.
(23) Höfer, P., Choi, Y. J., Osborne, M. J., Miguez, C. B., Vermette, P., and Groleau, D. (2010) Production of functionalized polyhydroxyalkanoates by genetically modified *Methylobacterium extorquens* strains. *Microb. Cell Fact. 9*, 1−13.
(24) FitzGerald, K. A., and Lidstrom, M. E. (2003) Overexpression of a heterologous protein, haloalkane dehalogenase, in a poly-beta-hydroxybutyrate-deficient strain of the facultative methylotroph *Methylobacterium extorquens* AM1. *Biotechnol. Bioeng. 81*, 263−268.
(25) Liu, Q., Kirchhoff, J. R., Faehnle, C. R., Viola, R. E., and Hudson, R. A. (2006) A rapid method for the purification of methanol dehydrogenase from *Methylobacterium extorquens*. *Protein Expression Purif. 46*, 316−320.
(26) Chubiz, L. M., Purswani, J., Carroll, S. M., and Marx, C. J. (2013) A novel pair of inducible expression vectors for use in Methylobacterium extorquens. *BMC Res. Notes 6*, 183.
(27) Choi, Y. J., Morel, L., Bourque, D., Mullick, A., Massie, B., and Miguez, C. B. (2006) Bestowing inducibility on the cloned methanol dehydrogenase promoter (PmxaF) of *Methylobacterium extorquens* by applying regulatory elements of *Pseudomonas putida* F1. *Appl. Environ. Microbiol. 72*, 7723−7729.
(28) Silva-Rocha, R., Martinez-Garcia, E., Calles, B., Chavarria, M., Arce-Rodriguez, A., de las Heras, A., Paez-Espino, A. D., Durante-Rodriguez, G., Kim, J., Nikel, P. I., Platero, R., and de Lorenzo, V. (2013) The Standard European Vector Architecture (SEVA): a coherent platform for the analysis and deployment of complex prokaryotic phenotypes. *Nucleic Acids Res. 41*, D666−D675.
(29) Kaczmarczyk, A., Campagne, S., Danza, F., Metzger, L. C., Vorholt, J. A., and Francez-Charlot, A. (2011) Role of *Sphingomonas* sp. strain Fr1 PhyR-NepR-σEcfG cascade in general stress response and identification of a negative regulator of PhyR. *J. Bacteriol. 193*, 6629−6638.
(30) Okubo, Y., Skovran, E., Guo, X. F., Sivam, D., and Lidstrom, M. E. (2007) Implementation of microarrays for *Methylobacterium extorquens* AM1. *Omics 11*, 325−340.
(31) Frohman, M. A., Dush, M. K., and Martin, G. R. (1988) Rapid production of full-length cDNAs from rare transcripts: amplification using a single gene-specific oligonucleotide primer. *Proc. Natl. Acad. Sci. U.S.A. 85*, 8998−9002.

(32) Solovyev, V., and Salamov, A. (2011) Automatic annotation of microbial genomes and metagenomic sequences, In *Metagenomics and Its Applications in Agriculture, Biomedicine, and Environmental Studies* (Li, R. W., Ed.) pp 61−78, Nova Science Publishers, Hauppauge, NY.
(33) Leveau, J. H. J., and Lindow, S. E. (2001) Predictive and interpretive simulation of green fluorescent protein expression in reporter bacteria. *J. Bacteriol. 183*, 6752−6762.
(34) Hansen, L. H., and Sørensen, S. J. (2001) The use of whole-cell biosensors to detect and quantify compounds or conditions affecting biological systems. *Microb. Ecol. 42*, 483−494.
(35) Davidson, C. J., and Surette, M. G. (2008) Individuality in bacteria. *Annu. Rev. Genet. 42*, 253−268.
(36) Cormack, B. P., Valdivia, R. H., and Falkow, S. (1996) FACS-optimized mutants of the green fluorescent protein (GFP). *Gene 173*, 33−38.
(37) Choi, K. H., and Schweizer, H. P. (2006) mini-Tn7 insertion in bacteria with single attTn7 sites: example *Pseudomonas aeruginosa*. *Nat. Protoc. 1*, 153−161.
(38) Shaner, N. C., Campbell, R. E., Steinbach, P. A., Giepmans, B. N. G., Palmer, A. E., and Tsien, R. Y. (2004) Improved monomeric red, orange and yellow fluorescent proteins derived from *Discosoma* sp red fluorescent protein. *Nat. Biotechnol. 22*, 1567−1572.
(39) Erb, T. J., Berg, I. A., Brecht, V., Müller, M., Fuchs, G., and Alber, B. E. (2007) Synthesis of C5-dicarboxylic acids from C2-units involving crotonyl-CoA carboxylase/reductase: the ethylmalonyl-CoA pathway. *Proc. Natl. Acad. Sci. U.S.A. 104*, 10631−10636.
(40) Chistoserdova, L. V., and Lidstrom, M. E. (1996) Molecular characterization of a chromosomal region involved in the oxidation of acetyl-CoA to glyoxylate in the isocitrate-lyase-negative methylotroph *Methylobacterium extorquens* AM1. *Microbiology 142*, 1459−1468.
(41) Marx, C. J., and Lidstrom, M. E. (2001) Development of improved versatile broad-host-range vectors for use in methylotrophs and other Gram-negative bacteria. *Microbiology 147*, 2065−2075.
(42) Lim, H. N., Lee, Y., and Hussein, R. (2011) Fundamental relationship between operon organization and gene expression. *Proc. Natl. Acad. Sci. U.S.A. 108*, 10626−10631.
(43) Alber, B. E. (2011) Biotechnological potential of the ethylmalonyl-CoA pathway. *Appl. Microbiol. Biotechnol. 89*, 17−25.
(44) Sonntag, F., Buchhaupt, M., and Schrader, J. (2014) Thioesterases for ethylmalonyl-CoA pathway derived dicarboxylic acid production in *Methylobacterium extorquens* AM1. *Appl. Microbiol. Biotechnol. 98*, 4533−4544.
(45) Okubo, Y., Yang, S., Chistoserdova, L., and Lidstrom, M. E. (2010) Alternative route for glyoxylate consumption during growth on two-carbon compounds by *Methylobacterium extorquens* AM1. *J. Bacteriol. 192*, 1813−1823.
(46) Schneider, K., Skovran, E., and Vorholt, J. A. (2012) Oxalyl-coenzyme A reduction to glyoxylate is the preferred route of oxalate assimilation in *Methylobacterium extorquens* AM1. *J. Bacteriol. 194*, 3144−3155.
(47) Suarez, A., Güttler, A., Strätz, M., Staendner, L. H., Timmis, K. N., and Guzmán, C. A. (1997) Green fluorescent protein-based reporter systems for genetic analysis of bacteria including monocopy applications. *Gene 196*, 69−74.
(48) Marx, C. J., and Lidstrom, M. E. (2002) Broad-host-range cre-lox system for antibiotic marker recycling in Gram-negative bacteria. *Biotechniques 33*, 1062−1067.
(49) Peel, D., and Quayle, J. (1961) Microbial growth on C1 compounds. 1. Isolation and characterization of *Pseudomonas* AM1. *Biochem. J. 81*, 465.
(50) Peyraud, R., Kiefer, P., Christen, P., Massou, S., Portais, J.-C., and Vorholt, J. A. (2009) Demonstration of the ethylmalonyl-CoA pathway by using ^{13}C metabolomics. *Proc. Natl. Acad. Sci. U.S.A. 106*, 4846−4851.
(51) Kaczmarczyk, A., Vorholt, J. A., and Francez-Charlot, A. (2013) Cumate-inducible gene expression system for sphingomonads and other Alphaproteobacteria. *Appl. Environ. Microbiol. 79*, 6795−6802.
(52) Mesa, S., Hauser, F., Friberg, M., Malaguti, E., Fischer, H. M., and Hennecke, H. (2008) Comprehensive assessment of the regulons controlled by the FixLJ-FixK2-FixK1 cascade in *Bradyrhizobium japonicum*. *J. Bacteriol. 190*, 6568−6579.
(53) Simon, R., Priefer, U., and Puhler, A. (1983) A broad host range mobilization system for *in vivo* genetic-engineering—transposon mutagenesis in Gram-negative bacteria. *Nat. Biotechnol. 1*, 784−791.
(54) Kaczmarczyk, A., Vorholt, J. A., and Francez-Charlot, A. (2012) Markerless gene deletion system for sphingomonads. *Appl. Environ. Microbiol. 78*, 3774−3777.
(55) Sambrook, J., and Russell, D. W. (2001) *Molecular Cloning: A Laboratory Manual*, Cold Spring Harbor Laboratory Press, Cold Spring Harbor, NY.
(56) Toyama, H., Anthony, C., and Lidstrom, M. E. (1998) Construction of insertion and deletion mxa mutants of *Methylobacterium extorquens* AM1 by electroporation. *FEMS Microbiol. Lett 166*, 1−7.
(57) Andersen, J. B., Sternberg, C., Poulsen, L. K., Bjorn, S. P., Givskov, M., and Molin, S. (1998) New unstable variants of green fluorescent protein for studies of transient gene expression in bacteria. *Appl. Environ. Microbiol. 64*, 2240−2246.
(58) Lagendijk, E. L., Validov, S., Lamers, G. E., de Weert, S., and Bloemberg, G. V. (2010) Genetic tools for tagging Gram-negative bacteria with mCherry for visualization *in vitro* and in natural habitats, biofilm and pathogenicity studies. *FEMS Microbiol. Lett. 305*, 81−90.
(59) Erb, T. J. (2009) The ethylmalonyl-CoA pathway—a novel acetyl-CoA assimilation strategy. Ph.D.Thesis, Albert-Ludwigs-Universität Freiburg, Germany.
(60) Gibson, D. G., Young, L., Chuang, R. Y., Venter, J. C., Hutchison, C. A., 3rd, and Smith, H. O. (2009) Enzymatic assembly of DNA molecules up to several hundred kilobases. *Nat. Methods 6*, 343−345.
(61) Amann, R. I., Binder, B. J., Olson, R. J., Chisholm, S. W., Devereux, R., and Stahl, D. A. (1990) Combination of 16S rRNA-targeted oligonucleotide probes with flow cytometry for analyzing mixed microbial populations. *Appl. Environ. Microbiol. 56*, 1919−1925.
(62) Schindelin, J., Arganda-Carreras, I., Frise, E., Kaynig, V., Longair, M., Pietzsch, T., Preibisch, S., Rueden, C., Saalfeld, S., Schmid, B., Tinevez, J. Y., White, D. J., Hartenstein, V., Eliceiri, K., Tomancak, P., and Cardona, A. (2012) Fiji: an open-source platform for biological-image analysis. *Nat. Methods 9*, 676−682.
(63) Gourion, B., Francez-Charlot, A., and Vorholt, J. A. (2008) PhyR is involved in the general stress response of *Methylobacterium extorquens* AM1. *J. Bacteriol. 190*, 1027−1035.
(64) Kiefer, P., Buchhaupt, M., Christen, P., Kaup, B., Schrader, J., and Vorholt, J. A. (2009) Metabolite profiling uncovers plasmid-induced cobalt limitation under methylotrophic growth conditions. *PLoS One 4*, e7831.
(65) Chung, S. T., Tan, R. T., and Suzuki, I. (1971) Glyoxylate carboligase of *Pseudomonas oxalaticus*. A possible structural role for flavine-adenine dinucleotide. *Biochemistry 10*, 1205−1209.
(66) Ornston, M. K., and Ornston, L. N. (1969) Two forms of D-glycerate kinase in *Escherichia coli*. *J. Bacteriol. 97*, 1227−1233.
(67) Bradford, M. M. (1976) A rapid and sensitive method for the quantitation of microgram quantities of protein utilizing the principle of protein-dye binding. *Anal. Biochem. 72*, 248−254.
(68) Schneider, K., Peyraud, R., Kiefer, P., Christen, P., Delmotte, N., Massou, S., Portais, J. C., and Vorholt, J. A. (2012) The ethylmalonyl-CoA pathway is used in place of the glyoxylate cycle by *Methylobacterium extorquens* AM1 during growth on acetate. *J. Biol. Chem. 287*, 757−766.
(69) Smith, E. F., and Townsend, C. O. (1907) A plant-tumor of bacterial origin. *Science 25*, 671−673.
(70) Poindexter, J. S. (1964) Biological properties and classification of the caulobacter group. *Bacteriol. Rev. 28*, 231−295.
(71) Innerebner, G., Knief, C., and Vorholt, J. A. (2011) Protection of Arabidopsis thaliana against Leaf-Pathogenic Pseudomonas syringae by Sphingomonas Strains in a Controlled Model System. *Appl. Environ. Microbiol. 77*, 3202−3210.

(72) Rivas, R., Abril, A., Trujillo, M. E., and Velazquez, E. (2004) Sphingomonas phyllosphaerae sp. nov., from the phyllosphere of Acacia caven in Argentina. *Int. J. Syst. Evol. Microbiol. 54*, 2147−2150.
(73) Yabuuchi, E., Yamamoto, H., Terakubo, S., Okamura, N., Naka, T., Fujiwara, N., Kobayashi, K., Kosako, Y., and Hiraishi, A. (2001) Proposal of *Sphingomonas wittichii* sp. nov. for strain RW1T, known as a dibenzo-*p*-dioxin metabolizer. *Int. J. Syst. Evol. Microbiol. 51*, 281−292.
(74) Regensburger, B., and Hennecke, H. (1983) RNA polymerase from *Rhizobium japonicum*. *Arch. Microbiol. 135*, 103−109.
(75) Smejkalova, H., Erb, T. J., and Fuchs, G. (2010) Methanol assimilation in *Methylobacterium extorquens* AM1: demonstration of all enzymes and their regulation. *PLoS One 5*, e13001.